Reusable shuttles for exchangeable functional cargos: reversibly assembled, magnetically powered organocatalysts for asymmetric aldol reactions

Carolina Mendoza[a,†] , Augustin de la Croix[a], Paola Riente[a,‡], Lluís Llorens [a,b], Javier de Mendoza[a,*] and Miquel A. Pericàs[a,*]

[a] *Institute of Chemical Research of Catalonia (ICIQ), The Barcelona Institute of Science and Technology, Avgda. Països Catalans, 16. E-43007 Tarragona, Spain. Fax: +34 977920244; Tel: +34 977920243*
[b]*Departament de Química Inorgànica i Orgànica, Universitat de Barcelona, c/ Martí i Franqués 1-11, E-08028 Barcelona, Spain.*

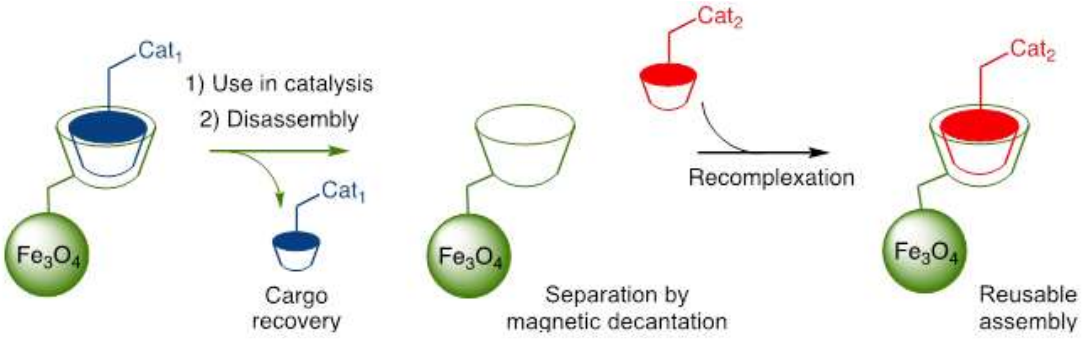

ARTICLE INFO

Article history:
Received
Received in revised form
Accepted
Available online

Keywords:
Aldol Reaction
Cyclodextrins
Nanoparticles
Organocatalysis
Recyclable Catalyst
Supramolecular Catalyst

ABSTRACT

A supramolecular approach has been followed to support adamantyl substituted proline organocatalysts onto the surface of magnetite nanoparticles decorated with a β-cyclodextrin motif. The resulting magnetic nanoparticles (*ca.* ~10 nm diameter) were used as modular, magnetically recyclable catalysts in the asymmetric aldol reaction of aromatic aldehydes with cyclic ketones in water. The catalytic assemblies can be easily dismantled in organic media, and the recovered nanoparticles (magnetically powered chemical shuttles) re-complexed with another suitably substituted catalytic unit (replaceable functional cargo).

1. Introduction

Shuttles have become popular in space exploration because they are (at least partially) reusable, thus significantly reducing the high cost of each mission. Similarly, chemical shuttles are desirable in a variety of areas, such as catalysis and drug delivery. In particular, shuttles are attractive when *translocation*, induced by an external physical or chemical stimulus, combines with *function*, such as a catalytic process, arising from another part of the molecule.

Immobilisation of asymmetric catalysts on non-soluble supports constitutes an attractive alternative to homogeneous catalysis, as it allows easy recovery and recycling.[1] Thus, a wide variety of support types have been used, such as soluble and insoluble polymers,[2] silica,[3] dendrimers,[4] as well as magnetic nanoparticles (MNPs).[5] Among these supports, nanoparticles can present the additional advantages of increased catalytic activity, due to the accumulation of active centres on their surface, and to enhanced enantiocontrol, due to the close similarity with purely homogeneous processes.[5b,6]

Presumably, due to reasons such as the avoidance of catalyst leaching, minimization of product contamination and the possibility of recovery and reuse, catalyst immobilization by covalent tethering has become prevalent, although non-covalent attachment modes, such as encapsulation, adsorption or electrostatic interactions have also been explored.[7] In any case, complex catalytic systems assembled by covalent immobilization suffer from important vulnerabilities arising from the non-applicability of the *shuttling* principle. Thus, any failure in operation leads to the loss of the vehicle and its cargo.

Nowadays, the most versatile and readily available chemical shuttles are magnetite nanoparticles, displaying controllable mobility under the stimulus of an external magnetic field, due to their superparamagnetism.[8] In addition, their outer surface, rich in hydroxyl groups can be readily functionalized by grafting with a variety of ω-substituted 1,1,1-trialkoxysilanes. A variety of functional units have been incorporated on magnetic nanoparticles by this approach, most frequently using click chemistry (Fig. 1a).[9]

The vulnerability of the covalent approach mentioned above could be in principle overcome through the integration of high-affinity complexing units onto the magnetic nanoparticles surface. In this way, magnetically-powered chemical shuttles would be constructed, and functional cargos for different applications could be sequentially introduced by simple complexation-decomplexation-recomplexation sequences involving, for instance, the β-cyclodextrin-adamantyl supramolecular interaction (Fig. 1b). In addition to the increased versatility of this approach, any possible deactivation of the functional unit could be easily remediated by a solvent-induced disassembly of the non-covalent construct that would leave the valuable magnetically-powered shuttle ready for reuse through simple complexation with fresh catalytic units.

Although crown ethers and polyamines have been previously immobilised onto magnetic nanoparticles,[10] we decided to focus on receptors with high affinities for organic molecules. This is the case for β-cyclodextrin (a naturally occurring cyclic array of seven D-glucopyranosyl subunits linked by α-1,4-glycosidic bonds), which strongly binds adamantyl derivatives in water (K_{ass} = 10^5-10^6 M^{-1}).[11,12] Due to their low price, water solubility, lack of toxicity and highly hydrophobic internal cavities, cyclodextrins (CDs) have been widely exploited in the food, cosmetics and pharmaceutical industries[13] When dissolved in an aqueous phase, the inner space of CDs provides a hydrophobic micro-environment. Thanks to this property, CDs have been widely employed as enzyme mimics[14] and in catalysis, either covalently attached to chiral catalysts to act on an included substrate,[15] or by complexing the catalyst inside the cavity to act on external substrates.[16] Driving forces for inclusion into CDs are mainly van der Waals forces, hydrophobic interactions, electronic effects and steric factors.[12b,17]

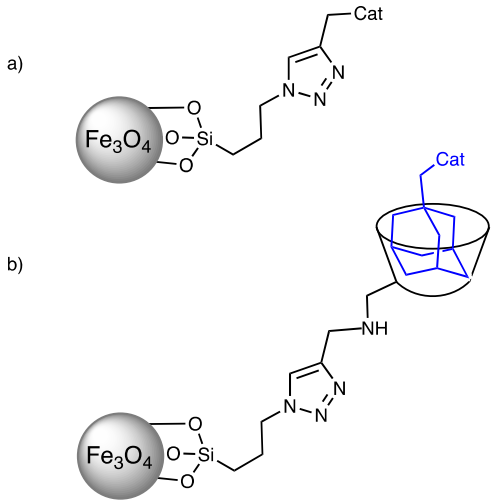

Figure 1. A single-purpose, magnetically powered catalyst (a) and a multipurpose, β-cyclodextrin-adamantyl reversibly assembled analogue designed to act as a chemical shuttle for a functional cargo (b).

CDs have also been attached to nanoparticles, for the adsorption of contaminants,[18] drug delivery[19] and catalysis.[20] Kaifer and co-workers reported the preparation of water-soluble CD-modified gold nanospheres forming host-guest complexes with ferrocenemethanol and 1-adamantanol.[21] Magnetic $Fe_{core}Pt_{shell}$ nanoparticles have also been modified with γ-CD (eight glucose subunits). The resulting water soluble nanoparticles have been employed as efficient catalysts for the aqueous hydrogenation of allyl alcohol[22] and, quite recently, MNPs decorated with β-CD were employed to recover an adamantyl-containing catalyst from the reaction medium.[23] However, a magnetically-powered catalytic shuttle with a catalytic cargo based on the β-CD-adamantyl interaction has not yet been reported in the literature.

In this work we describe a supramolecular approach to catalysis with immobilized systems that benefits from both covalent tethering and non-covalent attachment strategies as key elements of the shuttle design. This is based on the introduction of a supramolecular motif (namely, a cyclodextrin-adamantane contact) as a reversible linker between the magnetic nanoparticles and the catalyst molecule. This could allow the easy recovery of a given catalyst from the surface of the nanoparticle for the sequential use of different catalysts with the same shuttle (Fig. 2) or even exploring the operation of tandem catalytic effects with the simultaneous presence of different catalysts on the shuttle.[24] As a proof of concept for our design, we selected the proline catalysed aldol reaction between aromatic aldehydes and cyclohexanone in water. An adamantyl-decorated proline catalyst encapsulated into a β-CD has been reported by Liu and co-workers,[16b] yielding the corresponding hydroxyketones with high diastereo- and enantioselectivities.

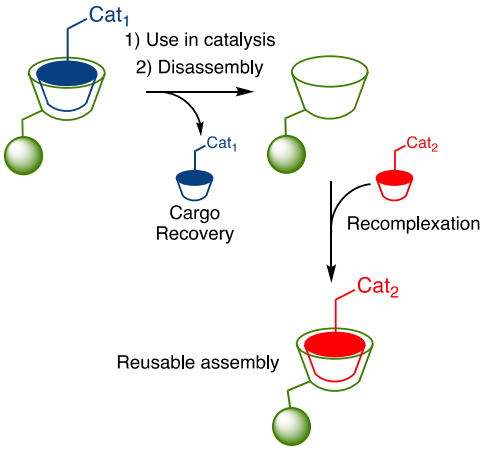

Figure 2. A multi-purpose, reversibly assembled magnetically powered catalyst for sequential use.

In our case, to attach the β-CD to the magnetic nanoparticles, we decided to prepare functional nanoparticles **1** (Fig. 3) incorporating a 1,2,3-triazole subunit in the linker, which can be easily formed through a copper-catalysed alkyne-azide cycloaddition (CuAAC) reaction,[25] the best known example of click chemistry.[26]

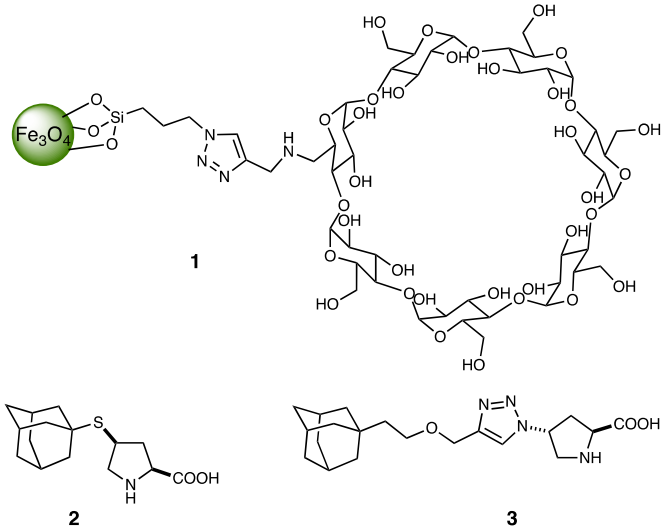

Figure 3. β-CD-functionalised MNPs (**1**) and partner L-hydroxyproline derivatives modified with adamantyl residues (**2** and **3**).

In recent years, we and other groups[27] have studied and established the validity of this approach for the immobilisation of catalytic species without negative effects on either the catalytic activity or stereoselectivity. As part of the ongoing work in our group on the preparation of functional ε-cobalt[28] and Fe_3O_4[9d-f, 29a-b] magnetic nanoparticles (MNPs) as easily recoverable and reusable catalysts, we decided to use azido-functionalised magnetite nanoparticles as platforms for the grafting of a monoalkynylated β-CD subunit through a "click" cycloaddition reaction. Two organocatalytic guests **2** and **3** were explored, differing mainly in the nature and length of the linker between the proline catalytic unit and the adamantyl anchor. While **2** was designed to behave as a loose guest due to the short distance between the hydrophobic moiety and the catalytic site, we considered that **3**, thanks to the longer linker connecting these two units, would lead to more tightly bound complexes with **1**. According to this design, **2** would serve as a proof of principle for the recoverability and recyclability of **1** (the chemical shuttle) should its catalytic cargo be lost by leaching.

2. Results and Discussion

*2.1. Synthesis and characterization of the catalytic materials **8-9** and **10-11***

MNPs of Fe_3O_4 (**4**) were prepared following the co-precipitation method, in the presence of oleic acid as a surfactant (Scheme 1).[30] Transmission electron microscopy (TEM) images revealed the formation of 8.4±2.6 nm nanoparticles (Fig. 4a). Next, the 3-azidopropyl moiety was grafted onto the surface of the MNPs by reaction with 3-azidopropyltrimethoxysilane (**5**) in toluene,[31] leading to 9.8±2.9 nm nanoparticles **6** (Fig. 4b) with a functionalization of approximately 0.30 mmol N_3/g (as determined by nitrogen elemental analysis).

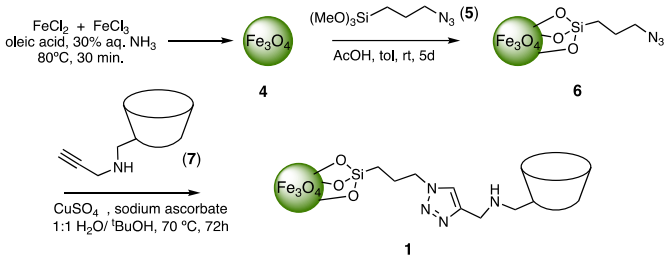

Scheme 1. Preparation of Fe_3O_4 MNPs **1** functionalised with β-CD.

Integration of the β-CD derivative **7**[32] onto the MNPs was carried out using a CuAAC reaction[25a-b] promoted by $CuSO_4$/sodium ascorbate, using a 1:1 water/*t*-butyl alcohol mixture as solvent. The reaction was monitored by IR spectroscopy (Fig. 5), and once the azide band of the functional nanoparticles (around 2097 cm^{-1}) had disappeared, the particles **1** were separated by magnetic decantation. The incorporation of the β-CD moiety was indicated by the presence of bands in the region of 900 - 1200 cm^{-1} associated with the C-O bonds in the IR spectrum of **1**. The evolution of the shape and size of the functional nanoparticles, from **4** to **1** was followed by TEM micrography (Fig. 4a-c) Nanoparticles **1** were obtained as a mixture of small aggregates and discrete particles with a diameter of 10.3±2.9 nm (Fig. 4c), without significant change in the aspect or size with respect to precursors **4** and **6**. The degree of functionalisation of MNPs **1** was determined by elemental analysis (%N) and found to have β-CD loadings of approximately 0.21 mmol/g.

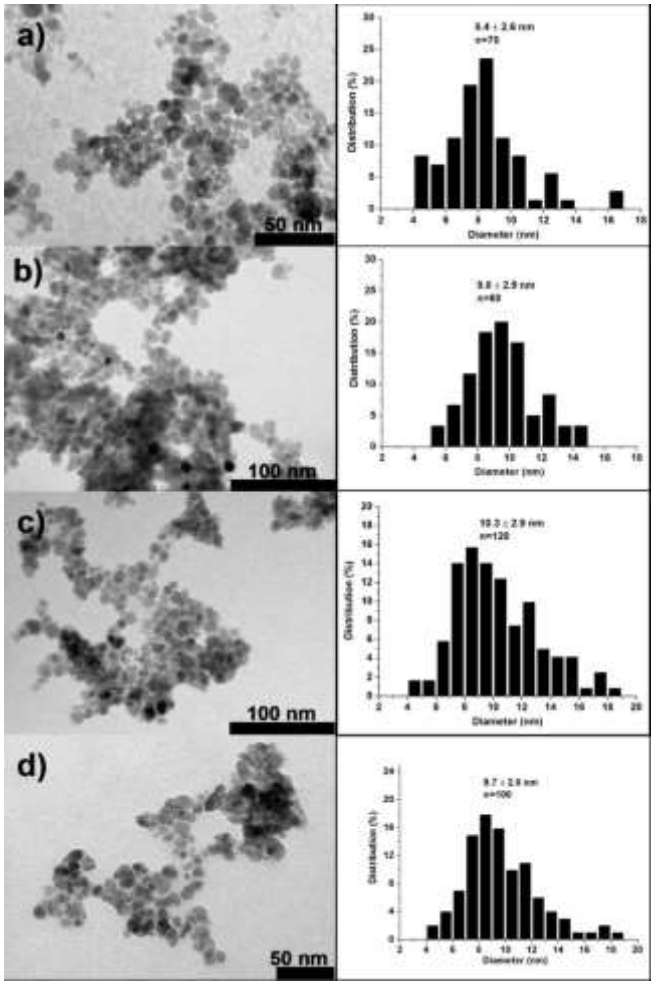

Figure 4. TEM image and size distribution of a) MNPs **4**, b) azide-functionalized MNPs **6**, c) β-CD-functionalised MNPs **1** and d) MNPs **11**.

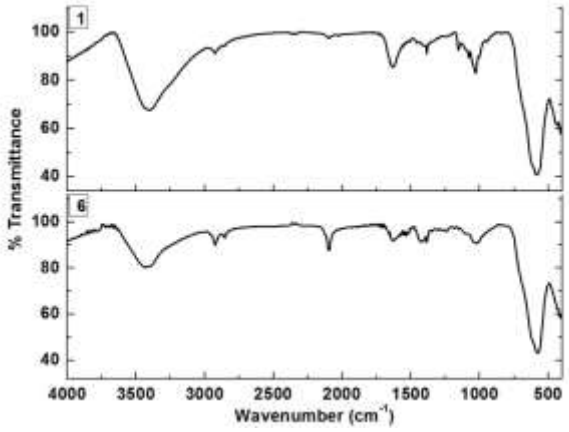

Figure 5. IR spectra of azide-functionalised MNPs **6** and β-CD-functionalised MNPs **1**.

To test the shuttling principle in catalysis, proline derivatives **2** and **3** (Fig. 3, see ESI for synthetic details) were first submitted to complexation with β-CD for comparative purposes (Scheme 2).

To this end, equimolar amounts of **2** or **3** and β-CD were dissolved in 95:5 water/methanol. The reaction mixture was stirred at room temperature for 2-48 h, and the solvent was then removed ununder reduced pressure to afford the corresponding complex **8** or **9**. Both ^{1}H NMR spectroscopy and MS provided evidence of the formation of the host-guest complexes (see ESI for NMR spectra). In the case of **8**, TOF-MS (positive mode) shows a peak at 1438.3 amu that was assigned to the cation $[M+Na]^{+}$, where M corresponds to the mass of the inclusion complex between β-CD and guest **2** ($C_{57}H_{93}N_4O_{37}S$). On the other hand, the TOF-MS spectrum (negative mode) of complex **9** shows a peak at *m/z* = 1507.3 amu, assigned to the anion $[M-H]^{-}$ where M is the mass of the inclusion complex between β-CD and guest **3**.

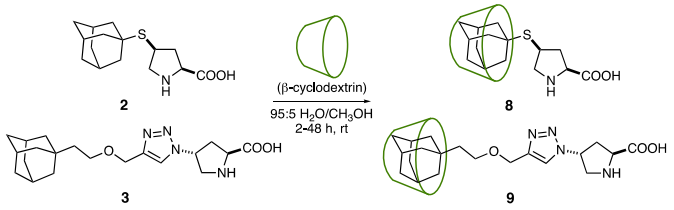

Scheme 2. Preparation of inclusion complexes of β-CD with L-proline derivatives **2** and **3**.

Following the same procedure, proline derivatives **2** and **3** were immobilised onto the surface of the cyclodextrin-modified magnetite nanoparticles **6** to provide the shuttle+catalyst nanoparticle assemblies **10** and **11** (Fig. 6).

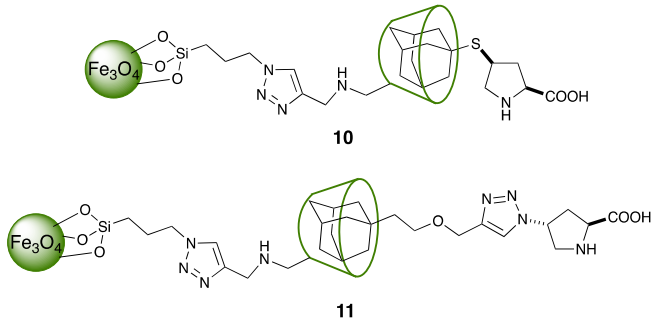

Figure 6. Fully assembled shuttle+catalyst nanoparticles **10** and **11**.

TEM images (Fig. 4d) showed that the size of the nanoparticles was maintained (9.1±2.2 nm for nanoparticles **10** and 9.7±2.8 nm for **11**).

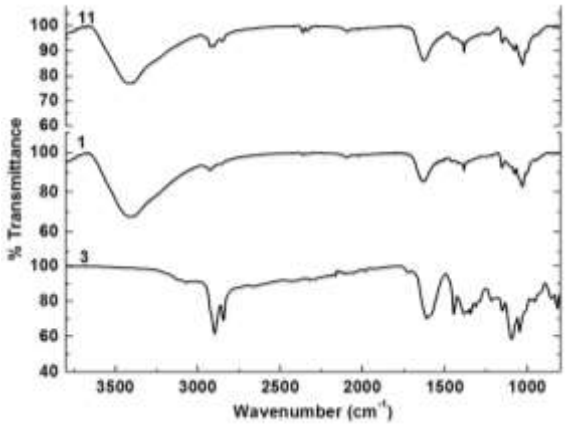

Figure 7. Comparison of the IR spectra of proline derivative **3**, MNPs **1** and MNPs **11**.

The appearance of an additional band at 2989 cm^{-1} in the IR spectrum of the assemblies (Fig. 7) supports the presence of the proline catalytic unit on the surface of the nanoparticles. Thermogravimetric analysis (Fig. 8), is also strongly indicative of the presence of the proline derivative on the surface of the nanoparticles. Thus, 25% of the initial weight is lost between 300 and 800 ºC from nanoparticles **11**, whereas a much lower weight

loss is recorded for β-CD-functionalised nanoparticles **1** over the same temperature range.

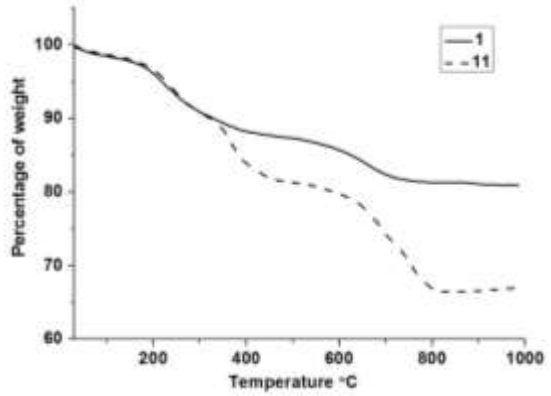

Figure 8. TGA curves showing the weight loss of nanoparticles **11** and **1** over the 300-800 ºC temperature range.

*2.2. Catalytic behaviour of **2-3** and **8-9** in the asymmetric aldol reaction in water*

We first evaluated prolines **2-3** as catalysts in the model asymmetric aldol reaction of benzaldehyde (**12a**) and cyclohexanone (**13**) in water, using 10 mol% of the catalyst (Table 1, entries 1 and 4). In both cases, moderate yields of the aldol product were obtained after 24 hours, with good to excellent enantioselectivities. In terms of diastereo- and enantioselectivity, the best results were recorded for catalyst **3** (>99% ee). The scope of these catalysts for different aldehydes and ketones was examined under the same conditions (see ESI) leading to results that are comparable with those recorded with analogous 4-hydroxyproline derivatives.[33] The β-CD complexes **8** and **9** were also tested for the same reaction using conditions analogous to the previous experiments (10 mol% of catalyst, 60 eq. of water and rt). Excellent stereoselectivities were observed for both catalysts (entries 6 and 7), although in the case of **8** a decrease in activity was observed with respect to the uncomplexed catalyst (compare entries 1 and 6). When catalyst **9** was allowed to react for 48 hours, a nearly complete conversion was achieved (compare entries 10 and 11). Overall, the results are very good both in terms of enantio- and diastereoselectivity. For catalyst **8** the enantioselectivity was improved for both **12a** and *p*-trifluoromethylbenzaldehyde (**12b**). In the case of **9** the results were very similar to those obtained for the uncomplexed proline **3**, both for **12a** and **12b**.

Table 1. Asymmetric aldol reaction of **12a-b** and **13** using proline derivatives **2** and **3**,[a)] β-CD complexes **8** and **9**,[b)] and functional nanoparticles **10** and **11**[c)] as catalysts.

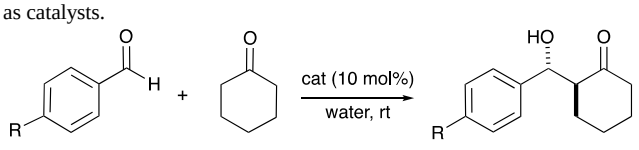

R = H **12a**
R = CF_3 **12b**

13

R = H **14a**
R = CF_3 **14b**

Entry	Catalyst	R	Time [h]	Yield [%][d)]	*anti:syn* [e)]	ee_{anti} [%][f)]
1	**2**	H	24	26	6:1	85
2	**2**	H	48	35	6:1	81
3	**2**	CF_3	24	77	10:1	93
4	**3**	H	24	41	18:1	>99
5	**3**	CF_3	24	81	30:1	97
6	**8**	H	24	13	4.5:1	94
7	**9**	H	24	54	14:1	99
8	**8**	CF_3	24	61	12:1	96
9	**8**	CF_3	48	75	10:1	96
10	**9**	CF_3	24	70	32:1	96
11	**9**	CF_3	48	98	33:1	99
12[g)]	**10**	CF_3	24	32	9:1	92
13	**10**	CF_3	72	49	9:1	91
14	**11**	CF_3	72	90	13:1	87
15	**11**	H	72	52	4:1	78

[a] **2** or **3** (0.04 mmol), **12a-b** (0.4 mmol), **13** (2.0 mmol), water (8 mmol. [b] **8** or **9** (0.032 mmol), **12a-b** (0.3 mmol), **13** (1.5 mmol), water (18 mmol). [c] **10** or **11** (0.016-0.020 mmol), **12a-b** (0.2 mmol), **13** (1.0 mmol), water (12 mmol). [d] Isolated yield of the combined diastereoisomers. [e] Determined by ^{1}H NMR spectroscopy. [f] Determined by chiral HPLC. [g] **12b** (0.06 mmol), **13** (0.3 mmol), water (3.6 mmol).

*2.3. Testing the shuttling principle with **10-11**. Recovery and reuse of the MNP+β-CD shuttle*

For the catalytic study, functional nanoparticles **10** and **11** were suspended in water (60 eq.) and tested in the asymmetric aldol reaction of *p*-trifluoromethylbenzaldehyde (**12b**) with **13** (Table 1, entries 12-14). With nanoparticles **10**, the aldol product was obtained in moderate yield (32%) after 24 hours (entry 12) and, even after 72 hours, complete conversion was not achieved (entry 13). Although this clearly indicates a significant decrease in the activity of the catalyst upon complexation, in terms of diastereo- and enantioselectivity the results are perfectly comparable with those obtained with the free catalyst **2** and with the molecular complex **8**. For catalyst **11** (entry 14) the reaction of *p*-trifluoromethylbenzaldehyde was achieved with excellent yield (90%) after 72 hours reaction, but both diastereo- and enantioselectivities were eroded with respect to the reference, free catalyst **3** or its molecular complex **9**.

As we have already mentioned, one of the main advantages associated with supporting a catalyst onto MNPs is the possibility of recovery by simple magnetic decantation and reuse. Through the assembling process, the magnetic properties of the supported nanoparticles are *transmitted* to the chiral catalyst they contain, becoming *magnetically powered*, and can be moved through a liquid phase or held within it by application of an external magnetic field. From the sustainability point of view, a catalyst loaded onto such a *chemical shuttle* can be separated from the reaction media and subsequently recovered and reused by magnetic decantation involving the simple application of inexpensive neodymium magnets to the walls of the reaction vessel. In addition, if decomplexation takes place upon repeated use or is provoked, for instance, by exposure of the complex to an organic medium, the most expensive part of the construct (the magnetic nanoparticles) can still be recovered by magnetic decantation and recomplexed (with either the same catalytic unit or with a different one) for further use.

To demonstrate the recyclability and reconfigurability of magnetic shuttle **1**, freshly prepared **10** was first used as the catalyst in four consecutive runs of the aldol reaction between *p*-trifluoromethylbenzaldehyde and cyclohexanone (Table 2, entries 1-4). Indeed, while the enantioselectivity of the reaction remained constant during the recycling, the yield progressively decreased. This unsatisfactory result is due the poor solubility of the aldol product **14b** in water, which requires the use of

water/alcohol mixtures to separate the aldol product from the catalytic nanoparticles. While **10** is stable in water, the work-up is responsible for substantial leaching of the catalytic unit **2** and for the associated catalyst deactivation. Gratifyingly, the recovery of the unloaded shuttle **1** after the fourth reaction cycle was essentially quantitative. The recovered nanoparticles **1** were washed with THF to secure the removal of residual **2**, dried under vacuum, and submitted to re-complexation with **3**. Recycling of catalyst **11** assembled in this manner proved to be much more rewarding (entries 5-7). As could be anticipated from the design of the catalytic unit **3**, involving a longer linker/spacer that improves the supramolecular interaction between the β-CD and the adamantyl subunits, catalyst **11** behaves as a more stable entity under the employed reaction and work-up conditions, allowing multiple recycling without significant deterioration of the catalytic performance. In this manner, a proof of the shuttling principle has been established, although further work would be required to make this approach competitive with covalent-based catalyst immobilization.

Table 2. Recycling and reconfiguration of magnetic shuttle **1**, from catalyst **10** to **11** in the aldol reaction of **12b** with **13**.[a]

Catalyst	Cycle	Time [h]	Yield [%][b]	*anti*:*syn*[c]	ee$_{anti}$ [%][d]
10	1	24	32	9:1	92
	2	24	17	9:1	93
	3	24	Traces	6:1	91
	4	24	Traces	6:1	92
11	5	72	89	14:1	89
	6	72	57	10:1	87
	7	72	35	5:1	85

[a] Reaction conditions for catalyst **10**: aldehyde (0.2 mmol), **13** (1.0 mmol), water (12 mmol), catalyst (8-10 mol%), room temperature, 24 h; reaction conditions for catalyst **11**: aldehyde (0.2 mmol), ketone (1.0 mmol), water (12 mmol), catalyst (8 mol%), room temperature, 72 h. [b] Isolated yield of the combined diastereoisomers. [c] Determined by ^{1}H NMR spectroscopy. [d] Determined by chiral HPLC.

3. Conclusion

In summary, we have shown that superparamagnetic magnetite nanoparticles functionalised with β-cyclodextrin *via* click chemistry are suitable hosts for the non-covalent immobilization of L-proline derivatives bearing adamantyl residues. The resulting nanoparticles were used as magnetically recoverable catalysts in the asymmetric aldol reaction of aromatic aldehydes with cyclohexanone in water, displaying high diastereo- and enantioselectivities. We have also shown that the reversibly- assembled catalysts can be easily disassembled in organic media, and that the recovered functional nanoparticles (*magnetically powered chemical shuttles*) can be re-complexed with a different catalytic guest. This paves the way for the development of multipurpose catalytic kits assembled through non-covalent, yet strong hydrophobic interactions between magnetic nanoparticles decorated with suitable hosts (acting as *chemical shuttles*) and catalytic units equipped with complementary guests (as *replaceable functional cargos*).

4. Experimental Section

4.1. General information

Unless otherwise stated, all commercial compounds were used as received without any further purification. Ultra pure water was obtained from an SG Water Ultra clear basic system, that provides water with a conductivity at 25ºC of 0.055 μS. NMR spectra were recorded on a Bruker Avance 400 Ultrashield NMR spectrometer at room temperature unless otherwise stated. For ^{1}H NMR all chemical shifts are reported in ppm relative to the proton resonance resulting from incomplete deuteration of the corresponding NMR solvent: CD_3OD (3.31 ppm), $CDCl_3$ (7.27 ppm) and CD_2Cl_2 (5.32 ppm). In the case of ^{13}C NMR spectra all chemical shifts are reported in ppm relative to the carbon resonance of the corresponding deuterated NMR solvent: CD_3OD (49.15 ppm), CD_2Cl_2 (54 ppm) and $CDCl_3$ (77.23 ppm). IR spectra were recorded on a Bruker Tensor 27 FTIR spectrometer fitted with an ATR cell. IR spectra of nanoparticles were recorded on a Thermo Nicolet 5700 FTIR spectrometer, using KBr pellets. Reactions under microwave irradiation were performed in a CEM Discover microwave synthesis apparatus using 10 mL vessels with septa for reactions performed at elevated temperatures and pressures. HPLC analyses were performed with Agilent Technologies HP-1100 or HP-1200 apparatus, equipped with UV detector or diode array detectors and MS detector respectively. Chiralcel OD-H 5 μm (0.46 cm × 25 cm), Chiralpak AD-H 5 μm (0.46 cm × 25 cm), Chiralpak AS-H 5 μm (0.46 cm × 25 cm), Chiralpak IC 5 μm (0.46 cm × 25 cm), Chiralpak IA 5 μm (0.46 cm × 25 cm), Chiralpak IB 5 μm (0.46 cm × 25 cm) chiral columns fitted with guard columns were used to separate enantiomers. For the determination of the experimental conditions for the analysis, pure racemic samples were prepared and used as standards. Elemental analyses were performed at Servei de Microanàlisi de l'Institut d'Investigacions Químiques i Ambientals de Barcelona (IIQAB) or at Centro de Microanálisis Elemental, Departamento de Química Farmacéutica, Facultad de Farmacia de la Universidad Complutense de Madrid. Transmission electron microscopy (TEM) images were obtained with a JEOL JEM-1011 transmission electron microscope equipped with a lanthanum hexaboride filament operated at an acceleration voltage of 100 kV. Thermogravimetric analysis were performed in a Mettler Toledo TGA/SDTA 851^e thermo balance, working in a range of temperatures from room temperature to 1000 ºC, with a precision of ± 0.25 %. TGA results in the product description were recorded under nitrogen stream (80 mL/min) and with a heating rate of 10 ºC/min. Alumina crucibles of 100 μL of capacity were used.

*4.2. Preparation of magnetite nanoparticles coated with oleic acid (**4**)*

These nanoparticles were prepared by slight modifications of a previously reported procedure.[30] Iron(II) chloride tetrahydrate (99%) (3.01 g, 15 mmol) and iron(III) chloride hexahydrate (97%) (8.36 g, 30.0 mmol) were dissolved in degassed ultrapure water (140 mL) in a 500 mL round-bottomed flask and heated to 80 ºC, shaking vigorously with a shaker. Oleic acid (98%) (2.1 mmol, 0.60 g, 0.68 mL) dissolved in degassed acetone (15 mL) was added to the reaction mixture, followed by 30% aqueous NH_3 solution (18.2 mL). After this addition, further amounts of oleic acid were added (5 × 1.0 mL) over a 5 to 10 minutes period. The black reaction mixture was hold for 30 minutes at 80 ºC and then slowly cooled to room temperature. A 1:1 v/v mixture of methanol and acetone (100 mL) was then added to support the precipitation. After allowing the nanoparticles to settle overnight with the help of a magnet, the supernatant was separated using a cannula and the particles were washed with a 1:1 v/v mixture of methanol and acetone (5 × 100 mL). The nanoparticles were dried, first with an argon stream and then under vacuum. In this

manner, 3.8 g of nanoparticles were isolated as a dark brown solid. Particle size (n = 70, nm): 8.40 (*s* = 2.56); FT-IR (KBr): ν 3453, 3005, 2956, 2923, 2852, 1632, 1426, 1409, 1261, 1229, 1100, 1056, 802, 580 cm^{-1}.

*4.3. Preparation of 3-azidopropyltrimethoxysilane (**5**)*

This compound was prepared by slight modifications of a previously reported procedure.[31a] Sodium azide 95.5% (4.13 g, 60.7 mmol) was suspended in a mixture of anhydrous acetonitrile (80 mL, molecular sieves 4Å) and 2 mL DMF, under argon in a Schlenk flask. 3-iodopropyltrimethoxysilane 95% (5 mL, 24.3 mmol) was added with a syringe under stirring. The resulting white suspension was then stirred overnight at reflux. The reaction mixture was allowed to cool down to room temperature, the solvent was evaporated under reduced presure, dry pentane (45 mL) was added and the reaction mixture was stirred for 15 minutes. The pentane layer was transferred to another Schlenk flask using a cannula fitted with filter paper, a second addition of dry pentane was done and the process was repeated. The solvent was evaporated under reduced pressure to yield **5** (4.24 g, 20.7 mmol, 85% yield) as clear yellow liquid. All the spectroscopic data matched with those reported in the literature.[6] ^{1}H NMR (400 MHz, $CDCl_3$): δ 3.58 (s, 9H C*H*$_3$), 3.27 (t, ^3J(H-H) = 6.9 Hz, 2H), 1.77 – 1.67 (m, 2H), 0.75 – 0.66 ppm (m, 2H); ^{13}C NMR (100 MHz, $CDCl_3$) δ 53.9 (*C*H$_2$), 50.7 (*C*H$_3$), 22.7 (*C*H$_2$), 6.5 ppm (*C*H$_2$); FT-IR (ATR): *ν* 2942, 2841, 2094 (N_3), 1457, 1413, 1344, 1275, 1241, 1189, 1079, 883, 816, 628 cm^{-1}.

*4.4. Azido-functionalised magnetite nanoparticles (**6**)*

These nanoparticles were prepared by slight modifications of a previously reported procedure.[31c] In a typical preparation nanoparticles **4** (0.96 g) were dispersed by sonication (20 minutes) in about 480 mL of degassed toluene and then 3-azidopropyltrimethoxysilane **5** (1.92 g, 9.33 mmol) was added, followed by glacial acetic acid 99.5%, *d* = 1.05 g/mL (0.192 mL, 3.36 mmol) and ultrapure water (0.269 mL, 14.93 mmol). The reaction mixture was stirred at room temperature for 3.5 days. The black particles were allowed to settle overnight with the help of an external magnet. The supernatant was separated using a cannula, and the nanoparticles were washed with toluene (3 × 42 mL) and methanol (3 × 26 mL) and dried under vacuum. In this manner, 0.78 g of nanoparticles were recovered as a brown powder. According to the %N determined by elemental analysis the functionalization of the nanoparticles was *f* = 0.35 mmol N_3/g. Particle size: (n = 41, nm): 8.83 (*s* = 3.01); Found: C, 3.61; H, 0.80; N, 1.48; FT-IR (KBr): ν 3442, 2955, 2924, 2852, 2098 (N_3), 1637, 1420, 1239, 1182, 1103, 1022, 585 cm^{-1}.

*4.5. CuAAC reaction of alkyne (**7**) with azido-functionalised magnetite nanoparticles (**6**). Preparation of functional nanoparticles (**1**)*

Functional nanoparticles **6** (0.1 g, *f* = 0.283 mmol/g, 9.8±2.9 nm diameter) were dispersed in 8 mL of a 1:1 mixture of ultrapure water and *tert*-butyl alcohol in a 100 mL round bottomed flask using ultrasonication for 20 minutes. Alkyne **7** (0.066 g, 0.057 mmol) was added to the mixture, followed by the l-sodium ascorbate 99% (7.85 mg, 0.040 mmol) and copper(II) sulfate pentahydrate (0.919 mg, 3.68 μmol) as a solid. The reaction mixture was stirred at 70 ºC for 72 hours. Then the reaction was stopped and water was added to the reaction mixture. The particles were magnetically separated and washed as follows: water (5 mL), 20% v/v NH_4OH in water (2 mL), water (5 mL) and methanol (25 mL). The particles were dried *in vacuo* at 40 ºC. The nanoparticles (60 mg) were recovered as a brown solid. According to the %N determined by elemental analysis the functionalization of the nanoparticles was *f* = 0.123 mmol/g. Particle size: (n = 120, nm): 10.28 (*s*= 2.90); Found: C, 4.35; H, 0.93; N, 0.69; FT-IR (KBr): ν 3385, 2956, 2922, 2852, 1637, 1399, 1151, 1079, 1029, 581 cm^{-1}. TGA (30 – 1000 ºC, 10 ºC/min, under N_2; for a 2.7370 mg sample, % weight loss): 13.3668 (left imit: 99.28 ºC, right limit: 488.27 ºC), 3.9734 (left limit: 488.27 ºC, right limit: 847.22 ºC).

*4.6. Preparation of inclusion complexes of β-cyclodextrin with proline derivatives **2** and **3***

*4.6.1. Inclusion complex of β-cyclodextrin and compound **2**. Synthesis of complex **8***

β-Cyclodextrin (0.206 g, 0.178 mmol) was placed in a 500 mL round-bottomed flask and was dissolved in water (230 mL) to give a colourless solution. To this solution, **2** (0.050 g, 0.178 mmol) dissolved in methanol (12 mL) was added and the mixture was stirred at room temperature for two days. After this time, the solvents were evaporated under reduced pressure and the solid residue was dried *in vacuo* for 5 hours to render the title product **8** (0.219 g, 87% yield) as a white solid. When the complexation time was shortened to 2 hours, yield was 76%. ^{1}H NMR (400 MHz, D_2O): δ 5.11 (d, ^3J(H1,H2) = 3.4 Hz, 7H, *H*1 β-CD), 4.17 (m, 1H), 3.92 (m, 28H, *H*3 β-CD + *H*5 β-CD + *H*6 β-CD), 3.71 (dd, ^3J(H2-H3) = 9.8, ^3J(H1-H2) = 3.4 Hz, 7H, *H*2 β-CD), 3.63 (t, ^3J(H-H) = 9.3 Hz, 7H, *H*4 β-CD), 3.56 (m, 2H), 3.32 – 3.20 (m, 1H), 2.80 (m, 1H), 2.29 (m, 3H, C*H* adamantyl), 2.08 – 1.75 ppm (m, 13H, 6 × CH_2 adamantyl + C*H* proline); ^{13}C NMR (101 MHz, D_2O) δ 176.09 (*C*OOH), 104.92 (*C*H, C1 β-CD), 84.14 (*C*H, C4 β-CD), 75.86 (*C*H, C3 β-CD), 74.58 (*C*H, C2 + C5 β-CD), 63.21 (*C*H), 62.64 (*C*H$_2$, C6 β-CD), 56.83 (*C*H$_2$), 48.76 (*C*), 46.67 (*C*H$_2$), 40.18 (*C*H), 38.45 (*C*H$_2$), 38.30 (*C*H$_2$), 31.71 ppm (*C*H). FT-IR (ATR): ν 3279, 2910, 2851, 1624, 1449, 1367, 1329, 1299, 1245, 1152, 1101, 1079, 1022, 998, 936 cm^{-1}; MS (TOF MS ES+): *m/z* (%) 1438.3 (12 %) $[M+Na]^+$, 1157.2 (37 %) $[(β\text{-CD})+Na]^+$, 304.1 (100%) $[C_{15}H_{23}NO_2S+Na]^+$.

*4.6.2. Inclusion complex of β-cyclodextrin and compound **3**. Synthesis of complex **9***

β-cyclodextrin (0.085 g, 0.073 mmol) was placed in a 250 mL round-bottomed flask and was dissolved in water (94 mL) to give a colourless solution. To this solution, compound **3** (0.0275 g, 0.073 mmol) dissolved in methanol (7.1 mL) was added and the mixture was stirred at room temperature for two hours. After this time, the solvents were eliminated using a rotary evaporator and the solid residue was dried *in vacuo* for 5 hours to render the title product **9** (0.097 g, 88% yield) as a white solid. ^{1}H NMR (400 MHz, D_2O): δ 8.17 (s, 1H, H triazole), 5.65 – 5.48 (m, 1H), 5.10 (d, ^3J(H1-H2) = 3.6 Hz, 7H), 4.68 (s, 2H), 4.56 (t, *J*(H-H)= 8.8 Hz, 1H), 4.03 (m, 2H), 3.96 – 3.76 (m, 30H), 3.75 – 3.53 (m, 17H), 3.00 – 2.62 (m, 2H), 2.15 (s, 3H), 1.79 (m, 6H), 1.64 (s, 6H), 1.47 ppm (t, *J*(H-H) = 7.4 Hz, 2H). FT-IR (ATR): ν 3259, 2898, 2844, 1628, 1407, 1367, 1329, 1244, 1203, 1152, 1079, 1024, 998, 940, 846 cm^{-1}; MS (TOF MS ES$^-$): *m/z* (%) 1507.3 (52) $[M-H]^-$ ($C_{62}H_{99}N_4O_{38}$ requires 1507.59), 1133.1 (20) $[(β\text{-CD})-H]^-$, 373.1 (100) $[C_{20}H_{29}N_4O_3]^-$.

*4.7. Preparation of supramolecular complexes of functional magnetic nanoparticles 1 with proline derivatives **2** and **3***

*4.7.1. Catalytic magnetic nanoparticles **10***

Nanoparticles **1** (*f* = 0.14 mmol/g, 1.27 g, 0.141 mmol) were suspended in ultrapure water (278 mL) to give a brown suspension with sonication for 10 minutes. Proline derivative **2** (0.079 g, 0.282 mmol) was dissolved in methanol (14 mL) and was added to the nanoparticles dispersion. The mixture was stirred at room temperature for 48 hours. After this period, the nanoparticles were submitted to magnetic decantation, the

supernatant was separated and the particles washed with methanol (4 × 20 mL) to eliminate the excess of proline derivative **2**. Next, the functional nanoparticles were dried under vacuum, first in the vacuum line and then overnight at 40 ºC in a vacuum dessicator. In this manner, 1.18 g of nanoparticles were recovered. According to the %N determined by elemental analysis the functionalisation of the nanoparticles was *f* = 0.083 mmol/g. Particle size: (n = 32, nm): 9.08 (*s* = 2.23). Found: C, 6.34; H, 1.10; N, 0.58; S, 0.12. FT-IR (KBr): ν 3425, 2956, 2923, 2853, 1734, 1636, 1457, 1080, 1032, 582 cm^{-1}. TGA: (30 – 1000 ºC, 10 ºC/min, under N_2; for a 4.0470 mg sample, % weight loss): 14.3850 (left limit: 111.05 ºC, right limit: 477.63), 6.6399 (left limit: 476.66 ºC, right limit: 795.08), 7.2616 (left limit: 795.08 ºC, right limit: 923.61).

*4.7.2. Solvent-induced disassembly of functional magnetite nanoparticles **10***

Nanoparticles **10** (0.30 g) were suspended in anhydrous THF and stirred at room temperature for 2 hours. After this period, the nanoparticles were submitted to magnetic decantation, the supernatant was separated and the particles washed with anhydrous THF (5 mL). The organic phases were combined and evaporated under vacuum to afford amino acid **2** (7.4 mg, quantitative recovery) as an oil. The recovered nanoparticles were identical to MNPs **1** by IR.

*4.7.3. Preparation of functional nanoparticles **11***

Nanoparticles **1** (*f* = 0.13 mmol/g, 1.02 g, 0.146 mmol) were suspended in ultrapure water (100 mL) to give a brown suspension. The suspension was sonicated for 10 minutes, to ensure the dispersion of the nanoparticles. Proline derivative **3** (0.104 g, 0.277 mmol) was dissolved in 160 mL water with sonication and heating and was added to the nanoparticles dispersion. The mixture was stirred at room temperature for 48 hours. After this period the nanoparticles were magnetically separated and washed with water (5 × 30 mL) to eliminate the excess of proline derivative **3**. The solid material was dried under vacuum, first in the vacuum line and then overnight at 40 ºC in a vacuum dessicator. In this manner 0.941 g of nanoparticles were recovered as a brown solid. According to the %N determined by elemental analysis the functionalization of the nanoparticles was *f* = 0.094 mmol/g. Particle size: (n = 101, nm): 9.72 (*s* = 2.80). Found: C, 6.52; H, 1.09, N, 1.05. FT-IR (KBr): ν 3417, 2956, 2923, 2898, 2841, 1635, 1154, 1080, 1029, 584 cm^{-1}. TGA (30 – 1000 ºC, 10 ºC/min, under N_2; for a 4.7600 mg sample, % weight loss): 8.0172 (left limit: 129.34ºC, right limit: 318.32 ºC), 9.5587 (left limit: 320.27 ºC, right limit: 555.09 ºC), 7.2616 (left limit: 555.09 ºC, right limit: 719.23 ºC), 7.0041 (left limit: 719.23 ºC, right limit: 879.13 ºC).

4.8. Procedures for the asymmetric aldol reactions catalysed by β-cyclodextrin complexes

*4.8.1. With monomeric catalysts **8** and **9***

The catalyst **8** or **9** (0.032 mmol, 0.1 eq) was added to a suspension of the aldehyde **12** (0.3 mmol) and cyclohexanone **13** (155 µL, 1.5 mmol, 5 eq) in water (324 µL, 18 mmol, 60 eq). The reaction mixture was stirred for 24-48 hours at room temperature. After that, water (5 mL) was added and the aqueous layer was extracted with ethyl acetate (3 × 5 mL). The organic layer was dried with $MgSO_4$, filtered and concentrated in vacuo. The crude product was purified by silica gel column chromatography using 9:1 hexane-ethyl acetate as eluent.

*4.8.2. With functional magnetic nanoparticles **10** and **11***

The nanoparticles supported catalyst **10** or **11** (8-10 mol%) was suspended in water (216 µL, 12 mmol, 60 eq). Then to the suspension were added the aldehyde **12** (0.2 mmol) and cyclohexanone **13** (104 µL, 1.0 mmol, 5 eq). The reaction mixture was stirred at room temperature for 24-72h. Upon reaction, water (2 ml) and MeOH (3 ml) were subsequently added and the mixture was separated by magnetic decantation of the nanoparticles. The magnetic nanoparticles were subsequently rinsed with water (3 ml) and the aqueous layer together with the MeOH were extracted with ethyl acetate (3 × 5 mL). The organic layer was dried with anhydrous $MgSO_4$, filtrated and concentrated under reduced pressure. The crude product was purified by silica gel column chromatography using 9:1 hexane-ethyl acetate as eluent. The nanoparticles were then vortexed with additional water, decanted, dried and reused. To exchange the adsorbed catalyst, the magnetic nanoparticles were vortexed in THF (3 x 3 mL), magnetically decanted, rinsed with MeOH, water, and dried.

Dedication

This paper is warmly dedicated to Professor Stephen G. Davies, to honor his long standing commitment as an author and an editor in favor of asymmetric synthesis and asymmetric catalysis.

Acknowledgements

This work was funded by CERCA Programme-Generalitat de Catalunya and MINECO (grant CTQ2015-69136-R and Severo Ochoa Excellence Accreditation 2014-2018 [SEV-2013-0319]). C.M. thanks AGAUR for a predoctoral fellowship.

References

1. Trindade, A. F.; Gois, P. M. P.; Afonso, C. A. M. *Chem. Rev.* **2009,** *109*, 418-514.
2. a) Clot-Almenara, L.; Rodríguez-Escrich, C.; Osorio-Planes, L.; Pericàs, M. A. *ACS Catalysis* **2016,** *6*, 7647-7651; b) Izquierdo, J.; Pericàs, M. A. *ACS Catalysis* **2016,** *6*, 348-356; c) Sagamanova, I. K.; Sayalero, S.; Martinez-Arranz, S.; Albeniz, A. C.; Pericas, M. A. *Catalysis Science & Technology* **2015,** *5*, 754-764; d) Clark, J.; Mcquarrie, D., Eds. *Handbook of Green Chemistry & Technology*; Blackwell Publ.: London, 2002; e) Leadbeater, N. E.; Marco, M. *Chem. Rev.* **2002,** *102*, 3217-3274; f) McNamara, C. A.; Dixon, M. J.; Bradley, M. *Chem. Rev.* **2002,** *102*, 3275-3300; g) Buchmeiser, M. R., Ed. *Polymeric materials in organic synthesis and catalysis*; Wiley-VCH: Weinheim, 2003; h) Benaglia, M.; Puglisi, A.; Cozzi, F. *Chem. Rev.* **2003,** *103*, 3401-3429; i) Haag, R.; Roller, S. In *Top. Curr. Chem.;* Kirsching, A. Ed.; Springer: Heidelberg, 2004; j) Toy, P. H.; Shi, M. *Tetrahedron* **2005,** *61*, 12013; k) Dioos, B. M. L.; Vankelecom, I. F. J.; Jacobs, P. A. *Adv. Synth. Catal.* **2006,** *348*, 1413-1446; l) Cozzi, F. *Adv. Synth. Catal.* **2006,** *348*, 1367-1390; m) Itsuno, S.; Haraguchi, N. In *Handbook of Asymmetric Heterogeneous Catalysis;* Ding, K.; Uozumi, Y. Eds.; Wiley-VCH: Weinheim, 2008; n) Benaglia, M., Ed. *Recoverable and Recyclable Catalysts*; John Wiley &

Sons: Chichester, 2009; o) Lu, J.; Toy, P. H. *Chem. Rev.* **2009,** *109*, 815-838; p) Kristensen, T. E.; Hansen, T. *Eur. J. Org. Chem.* **2010,** *2010*, 3179-3204.
3. a) Han, B.; Zhao, L.; Song, Y.; Zhao, Z.; Yang, D.; Liu, R.; Liu, G. *Catalysis Science & Technology* **2018,** *8*, 2920-2927; b) Zamboulis, A.; Moitra, N.; Moreau, J. J. E.; Cattoen, X.; Wong Chi Man, M. *J. Mater. Chem.* **2010,** *20*, 9322-9338; c) Trewyn, B. G.; Hung-Ting, C.; Lin, V. S.-Y. In *Recoverable and Recyclable Catalysts;* Benaglia, M. Ed.; Wiley & Sons, Ltd., 2009; d) Zhao, Y.; Jin, R.; Chou, Y.; Li, Y.; Lin, J.; Liu, G. *RSC Advances* **2017,** *7*, 22592-22598.
4. a) Wu, L.; Liu, J.; Ma, B.; Fan, Q. In *Bridging Heterogeneous and Homogeneous Catalysis;* Can, L.; Yan, L. Eds.; Wiley VCH: Weinheim, 2014; b) Helms, B.; Fréchet, J. M. J. *Adv. Synth. Catal.* **2006,** *348*, 1125-1148.
5. a) Sreenivasarao, P.; Debasish, D.; Jyotirmayee, D. *Adv. Synth. Catal.* **2013,** *355*, 3532-3538; b) Jimeno, C.; Sayalero, S.; Pericàs, M. A. In *Heterogenized Homogeneous Catalysts for Fine Chemicals Production. Catalysis by Metal Complexes;* Barbaro, P.; Liguori, F. Eds.; Springer: Heidelberg, 2010; p. 123; c) Zaera, F. *Chem. Soc. Rev.* **2013,** *42*, 2746-2762; d) Dalpozzo, R. *Green Chem.* **2015,** *17*, 3671-3686; e) Wang, D.; Astruc, D. *Chem. Rev.* **2014,** *114*, 6949-6985.
6. Laurent, S.; Forge, D.; Port, M.; Roch, A.; Robic, C.; Elst, L. V.; Muller, R. N. *Chem. Rev.* **2008,** *108*, 2064-2110.
7. a) Zhi-Huai, L.; Zhi-Ming, Z.; Xiao-Yan, H.; Jun, Z.; Xiao, D.; Ying-Qiang, L. *Chirality* **2012,** *24*, 1092-1095; b) Fraile, J. M.; García, J. I.; Mayoral, J. A. *Chem. Rev.* **2008,** *109*, 360-417.
8. a) Stevens, P. D.; Li, G.; Fan, J.; Yen, M.; Gao, Y. *Chem. Commun.* **2005**, 4435-4437; b) Abu-Reziq, R.; Alper, H.; Wang, D.; Post, M. L. *J. Am. Chem. Soc.* **2006,** *128*, 5279-5282; c) Kawamura, M.; Sato, K. *Chem. Commun.* **2006**, 4718-4719; d) Shylesh, S.; Schünemann, V.; Thiel, W. R. *Angew. Chem.* **2010,** *122*, 3504-3537; e) Shylesh, S.; Schünemann, V.; Thiel, W. R. *Angew. Chem. Int. Ed.* **2010,** *49*, 3428-3459.
9. a) Luo, S. Z.; Zheng, X. X.; Cheng, J. P. *Chem. Commun.* **2008**, 5719-5721; b) Schatz, A.; Hager, M.; Reiser, O. *Adv. Funct. Mater.* **2009,** *19*, 2109-2115; c) Wang, B. G.; Ma, B. C.; Wang, Q. O.; Wang, W. *Adv. Synth. Catal.* **2010,** *352*, 2923-2928; d) Riente, P.; Yadav, J.; Pericàs, M. A. *Org. Lett.* **2012,** *14*, 3668-3671; e) Riente, P.; Mendoza, C.; Pericàs, M. A. *J. Mater. Chem.* **2011,** *21*, 7350-7355; f) Ranjbar, S.; Riente, P.; Rodríguez-Escrich, C.; Yadav, J.; Ramineni, K.; Pericàs, M. A. *Org. Lett.* **2016,** *18*, 1602-1605; g) Myung- Jong, J.; Dong- Hwan, L. *Angew. Chem.* **2010,** *122*, 1137-1140.
10. Mendoza, C.; Jansat, S.; Vilar, R.; Pericas, M. A. *RSC Advances* **2015,** *5*, 87352-87363.
11. Ueno, A. *Supramol. Sci.* **1996,** *3*, 31-36.
12. a) Szejtli, J. *Chem. Rev.* **1998,** *98*, 1743-1753; b) Hapiot, F.; Tilloy, S.; Monflier, E. *Chem. Rev.* **2006,** *106*, 767-781.
13. Hedges, A. R. *Chem. Rev.* **1998,** *98*, 2035-2044.
14. a) Breslow, R.; Doherty, J. B.; Guillot, G.; Lipsey, C. *J. Am. Chem. Soc.* **1978,** *100*, 3227-3229; b) Anslyn, E.; Breslow, R. *J. Am. Chem. Soc.* **1989,** *111*, 5972-5973; c) Anslyn, E.; Breslow, R. *J. Am. Chem. Soc.* **1989,** *111*, 8931-8932; d) Breslow, R.; Dong, S. D. *Chem. Rev.* **1998,** *98*, 1997-2011.
15. a) Schlatter, A.; Kundu, M. K.; Woggon, W. D. *Angew. Chem. Int. Ed.* **2004,** *43*, 6731-6734; b) Schlatter, A.; Kundu, M. K.; Woggon, W.-D. *Angew. Chem.* **2004,** *116*, 6899-6902.
16. a) Qi, M.; Tan, P. Z.; Xue, F.; Malhi, H. S.; Zhang, Z.-X.; Young, D. J.; Hor, T. S. A. *RSC Advances* **2015,** *5*, 3590-3596; b) Liu, K.; Haeussinger, D.; Woggon, W. D. *Synlett* **2007**, 2298-2300; c) Shen, Z. X.; Ma, J. M.; Liu, Y. H.; Jia, C. J.; Li, M.; Zhang, Y. W. *Chirality* **2005,** *17*, 556-558.
17. Rekharsky, M. V.; Inoue, Y. *Chem. Rev.* **1998,** *98*, 1875-1917.
18. a) Fuhrer, R.; Herrmann, I. K.; Athanassiou, E. K.; Grass, R. N.; Stark, W. J. *Langmuir* **2011,** *27*, 1924-1929; b) Kang, Y.; Zhou, L. L.; Li, X.; Yuan, J. Y. *J. Mater. Chem.* **2011,** *21*, 3704-3710; c) Badruddoza, A. Z. M.; Tay, A. S. H.; Tan, P. Y.; Hidajat, K.; Uddin, M. S. *J. Hazard. Mater.* **2011,** *185*, 1177-1186.
19. a) Banerjee, S. S.; Chen, D.-H. *Chem. Mater.* **2007,** *19*, 6345-6349; b) Banerjee, S. S.; Chen, D. H. *J. Nanopart. Res.* **2009,** *11*, 2071-2078.
20. a) Kiasat, A. R.; Nazari, S. *J. Mol. Catal. A: Chem.* **2012,** *365*, 80-86; b) Kaboudin, B.; Mostafalu, R.; Yokomatsu, T. *Green Chem.* **2013,** *15*, 2266-2274; c) Senra, J. D.; Malta, L. F. B.; da Costa, M.; Michel, R. C.; Aguiar, L. C. S.; Simas, A. B. C.; Antunes, O. A. C. *Adv. Synth. Catal.* **2009,** *351*, 2411-2422.
21. Liu, J.; Ong, W.; Roman, E.; Lynn, M. J.; Kaifer, A. E. *Langmuir* **2000,** *16*, 3000-3002.
22. Mori, K.; Yoshioka, N.; Kondo, Y.; Takeuchi, T.; Yamashita, H. *Green Chem.* **2009,** *11*, 1337-1342.
23. a) Li, Q.; Li, Y.; Wang, J.; Lin, Y.; Wei, Z.; Duan, H.; Yang, Q.; Bai, F.; Li, Y. *New J. Chem.* **2018,** *42*, 827-831; b) Qi, M.; Chew, B. K. J.; Yee, K. G.; Zhang, Z.-X.; Young, D. J.; Hor, T. S. A. *RSC Advances* **2016,** *6*, 23686-23692.
24. a) Wasilke, J.-C.; Obrey, S. J.; Baker, R. T.; Bazan, G. C. *Chem. Rev.* **2005,** *105*, 1001-1020; b) Lohr, T. L.; Marks, T. J. *Nature Chemistry* **2015,** *7*, 477.
25. a) Rostovtsev, V. V.; Green, L. G.; Fokin, V. V.; Sharpless, K. B. *Angew. Chem.* **2002,** *114*, 2708-2711; b) Rostovtsev, V. V.; Green, L. G.; Fokin, V. V.; Sharpless, K. B. *Angew. Chem. Int. Ed.* **2002,** *41*, 2596-2599; c) Tornøe, C. W.; Christensen, C.; Meldal, M. *The Journal of Organic Chemistry* **2002,** *67*, 3057-3064.
26. Kolb, H. C.; Finn, M. G.; Sharpless, K. B. *Angew. Chem. Int. Ed.* **2001,** *40*, 2004.
27. a) Gheorghe, A.; Matsuno, A.; Reiser, O. *Adv. Synth. Catal.* **2006,** *348*, 1016-1020; b) Font, D.; Jimeno, C.; Pericàs, M. A. *Org. Lett.* **2006,** *8*, 4653-4655; c) Font, D.; Sayalero, S.; Bastero, A.; Jimeno, C.; Pericàs, M. A. *Org. Lett.* **2008,** *10*, 337-340; d) Tilliet, M.; Lundgren, S.; Moberg, C.; Levacher, V. *Adv. Synth. Catal.* **2007,** *349*, 2079-2084; e) Fernandes, A. E.; Jonas, A. M.; Riant, O. *Tetrahedron* **2014,** *70*, 1709-1731.
28. a) Lagunas, A.; Jimeno, C.; Font, D.; Solà, L.; Pericàs, M. A. *Langmuir* **2006,** *22*, 3823-3829; b) Lagunas, A.; Mairata i Payeras, A.; Jimeno, C.; Puntes, V. F.; Pericàs, M. A. *Chem. Mater.* **2008,** *20*, 92-100; c) Michalek, F.; Lagunas, A.; Jimeno, C.; Pericàs, M. A. *J. Mater. Chem.* **2008,** *18*, 4692-4697; d) Eichenseer, C. M.; Kastl, B.;

Pericàs, M. A.; Hanson, P. R.; Reiser, O. *ACS Sustainable Chemistry & Engineering* **2016,** *4*, 2698-2705; e) Roy, S.; Pericas, M. A. *Org. Biomol. Chem.* **2009,** *7*, 2669-2677.

29. a) Vaquer, L.; Riente, P.; Sala, X.; Jansat, S.; Benet-Buchholz, J.; Llobet, A.; Pericas, M. A. *Catalysis Science & Technology* **2013,** *3*, 706-714; b) Mak, C. A.; Ranjbar, S.; Riente, P.; Rodríguez-Escrich, C.; Pericàs, M. A. *Tetrahedron* **2014,** *70*, 6169-6173.
30. Shen, L.; Laibinis, P. E.; Hatton, T. A. *Langmuir* **1999,** *15*, 447-453.
31. a) Bradley, C. A.; Yuhas, B. D.; McMurdo, M. J.; Tilley, T. D. *Chem. Mater.* **2009,** *21*, 174-185; b) Paoprasert, P.; Spalenka, J. W.; Peterson, D. L.; Ruther, R. E.; Hamers, R. J.; Evans, P. G.; Gopalan, P. *J. Mater. Chem.* **2010,** *20*, 2651-2658; c) De Palma, R.; Peeters, S.; Van Bael, M. J.; Van den Rul, H.; Bonroy, K.; Laureyn, W.; Mullens, J.; Borghs, G.; Maes, G. *Chem. Mater.* **2007,** *19*, 1821-1831.
32. a) Byun, H.-S.; Zhong, N.; Bittman, R. *Organic Syntheses* **2000,** *77*, 225; b) Guo, Z. M.; Jin, Y.; Liang, T.; Liu, Y. F.; Xu, Q.; Liang, X. M.; Lei, A. W. *J. Chromatogr. A* **2009,** *1216*, 257-263.
33. a) Hayashi, Y.; Sumiya, T.; Takahashi, J.; Gotoh, H.; Urushima, T.; Shoji, M. *Angew. Chem.* **2006,** *118*, 972-975; b) Hayashi, Y.; Sumiya, T.; Takahashi, J.; Gotoh, H.; Urushima, T.; Shoji, M. *Angew. Chem. Int. Ed.* **2006,** *45*, 958-961.